Electronic Supplementary Material (ESI) for Journal of Materials Chemistry A.

Supporting Information

High Catalytic Activity of Oxygen-vacancy-rich Tungsten Oxide Nanowires Supported by Nitrogen-doped Reduced Graphene Oxides for Hydrogen Evolution Reaction

Tadele Hunde Wondimu[1], Guan-Cheng Chen[1], Hsueh-Yu Chen[1], Daniel Manaye Kabtamu[1], Anteneh Wodaje Bayeh[1], Kai-Chin Wang[1], Hsin-Chih Huang[1], Chen-Hao Wang*[1,2]

[1]Department of Materials Science and Engineering, National Taiwan University of Science and Technology, Taipei 10607, Taiwan.

[2]Hierarchical Green-Energy Materials (Hi-GEM) Research Center, National Cheng Kung University, Tainan 70101, Taiwan

*Corresponding author, E-mail: chwang@mail.ntust.edu.tw

Tel: +886-2-2730-3715; Fax: +886-2-2737-6544

Figure S1 show calibration of our reference electrode (SCE) with RHE.

Therefore, from E(SCE) = 0242 + E Hg/Hg_2Cl_2 + 0.059*pH, SCE = 0.242 V

E(SCE) = 0242 + E Hg/Hg_2Cl_2 + 0.059*pH

E(RHE) = E(SCE) + E Hg/Hg_2Cl_2 + 0.059*pH ~ 0.260 V

E(RHE) = 0.260 V, the contribution of small voltage about 18 mV is may be from pH of 0.5 M H_2SO_4 and E Hg/Hg_2Cl_2.

E(RHE) = E(SCE) + 0.260 V

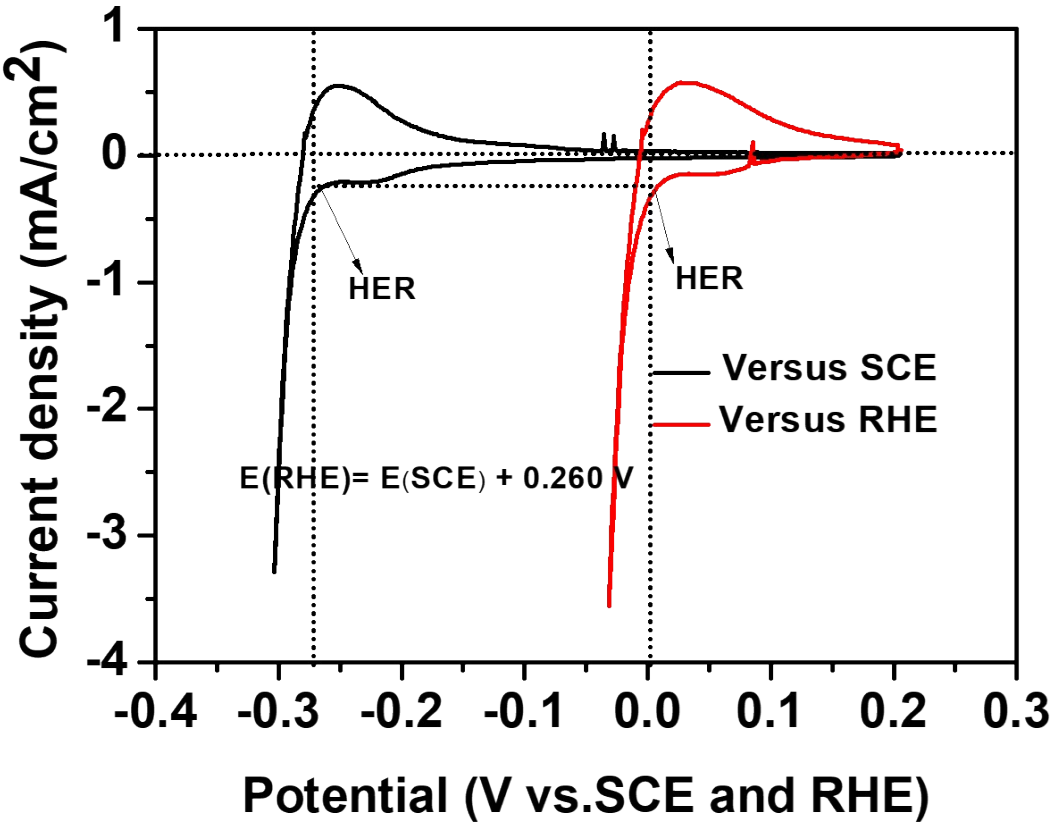

Figure S1 Cyclic Voltammetry calibration curve of SCE to RHE

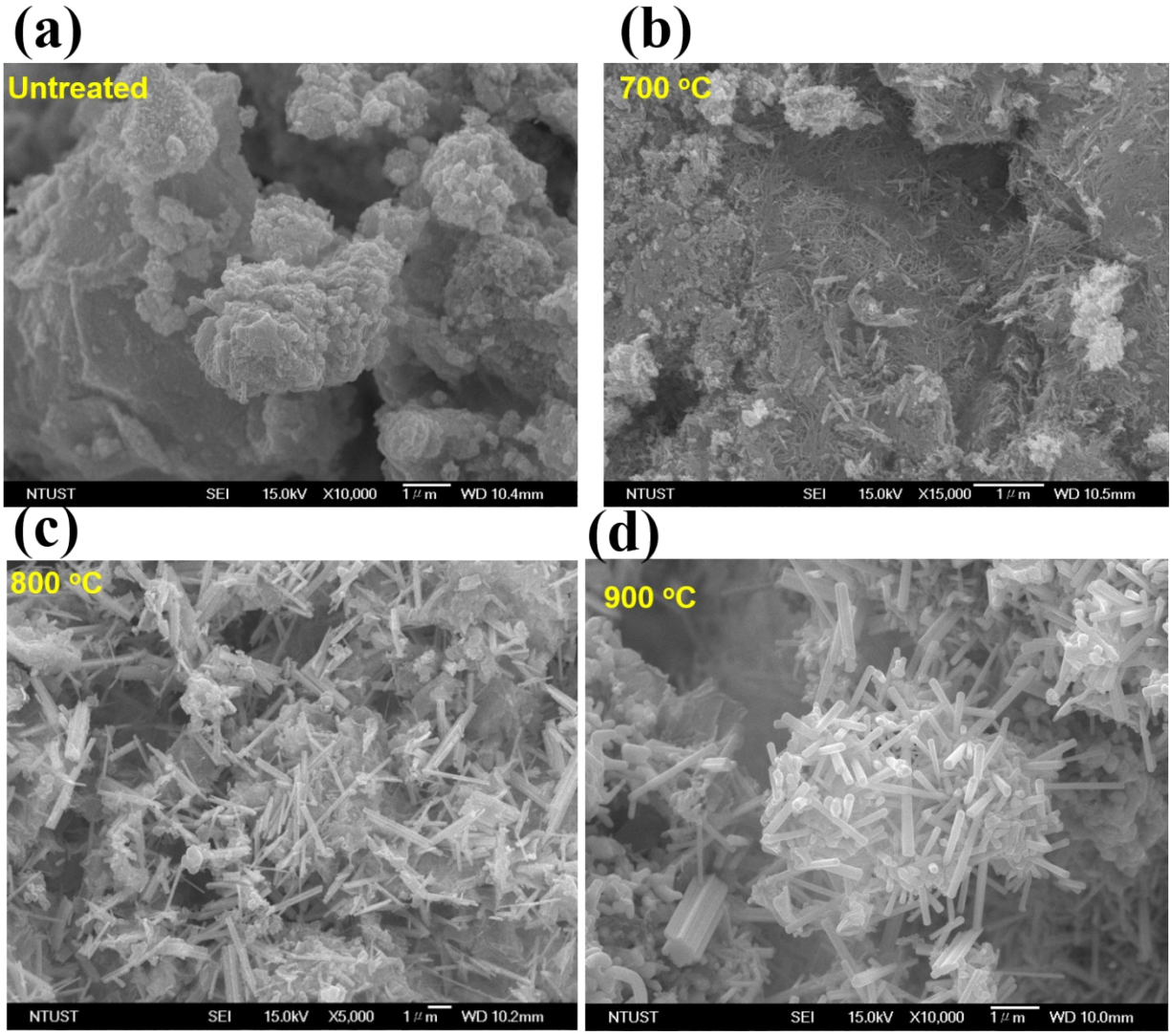

Figure S2 (a) SEM images of (a) untreated WOxNWs/N-rGO, **(b)** different heat treatment temperatures at (b) 700 °C , (c) 800 °C, and (d) 900 °C for WOxNWs/N-rGO.

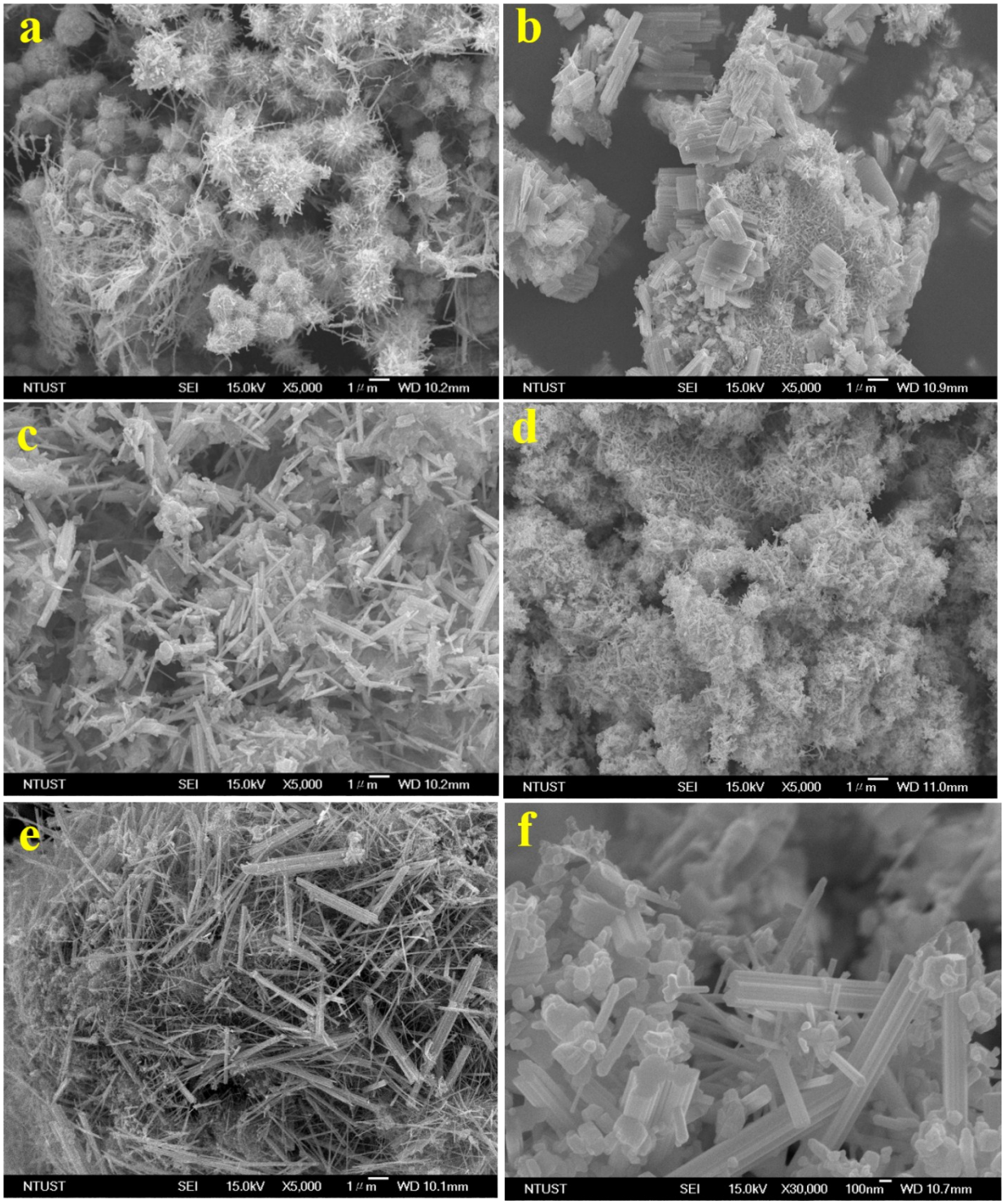

Figure S3 SEM images of the catalyst synthesized with glycerol for (a) WOxNWs (c) WOxNWs/rGO , and (e) WOxNWs/N-rGO, and without addition of glycerol for (b) WOxNWs, (d) WOxNWs/rGO, and (f) WOxNWs/N-rGO.

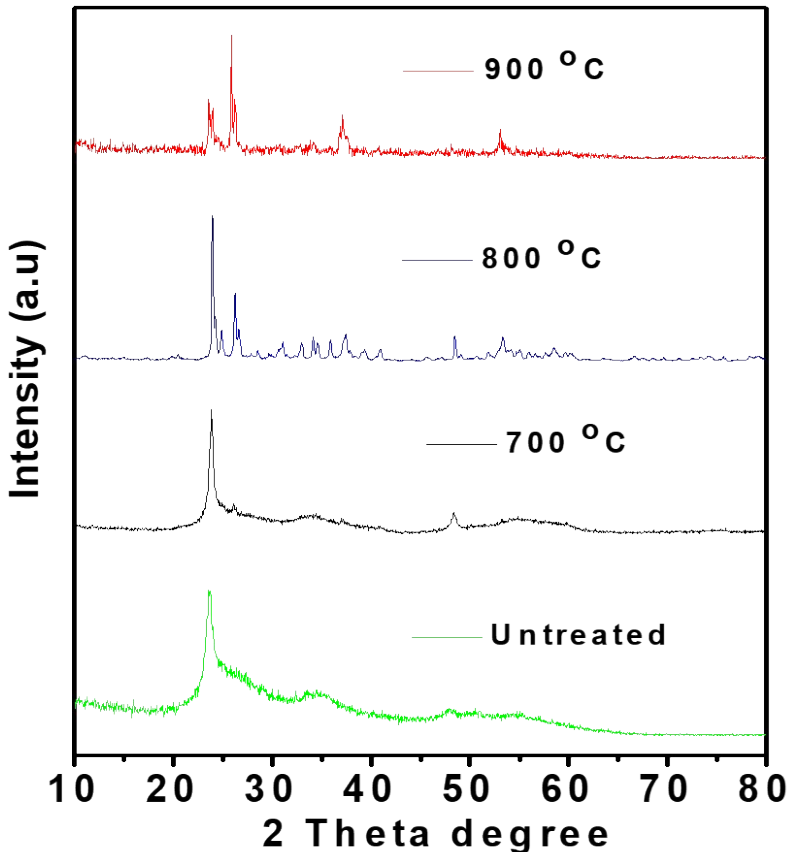

Figure S4 XRD patterns of WOxNWs/N-rGO at different annealing temperatures.

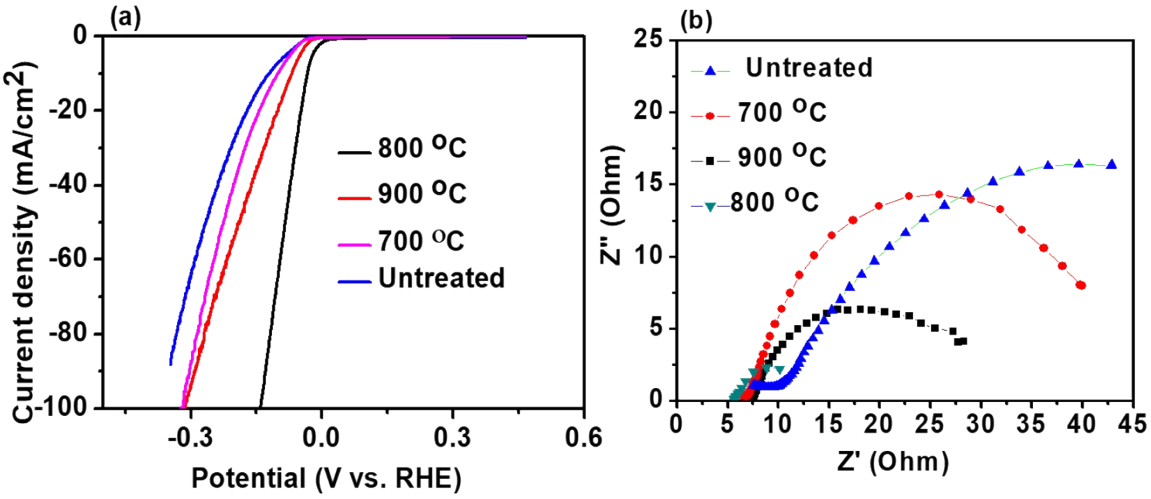

Figure S5 (a) Polarization curves and (b) EIS spectra of WOxNWs/N-rGO at different annealing temperatures.

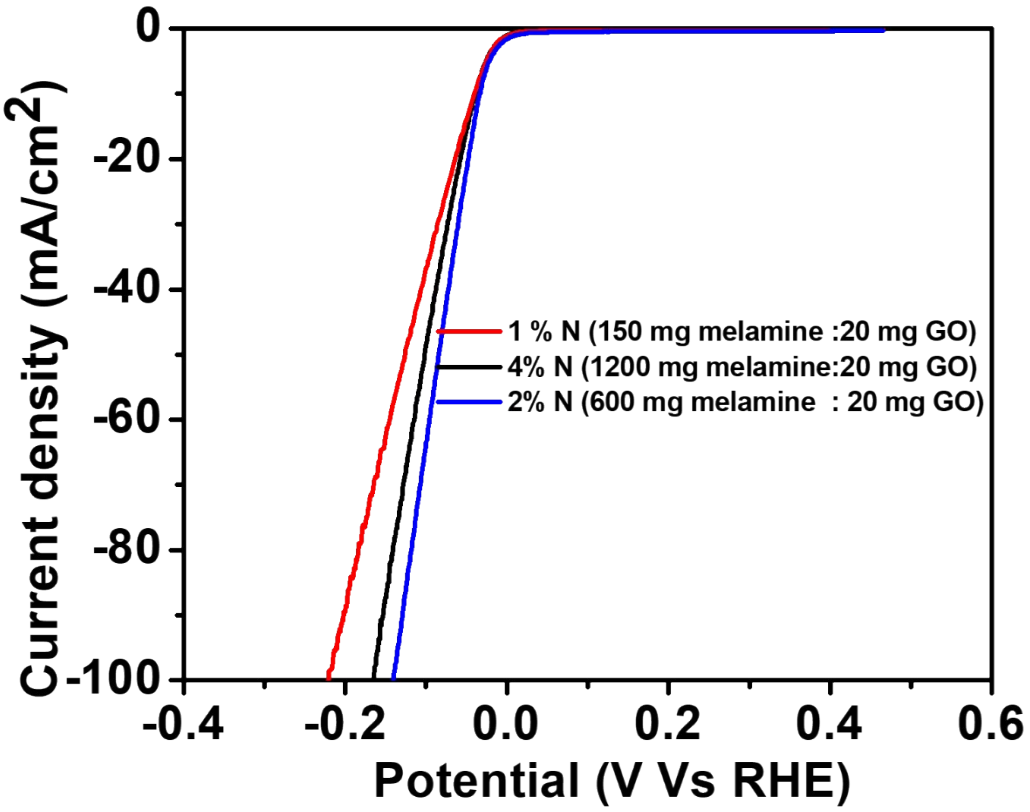

Figure S6 The effect of melamine amount or % N for HER activity of WOxNWs/N-rGO

In addition of XPS and Raman the presence of oxygen vacancies were investigated by UV-Vis. as clearly depicted in **Figure S7**. The WOxNWs/N-rGO shows a large absorption tail in the range of 500−1000 nm, strongly demonstrating the existence of a large amount of oxygen vacancies in WOxNWs/N-rGO compared to other composites.

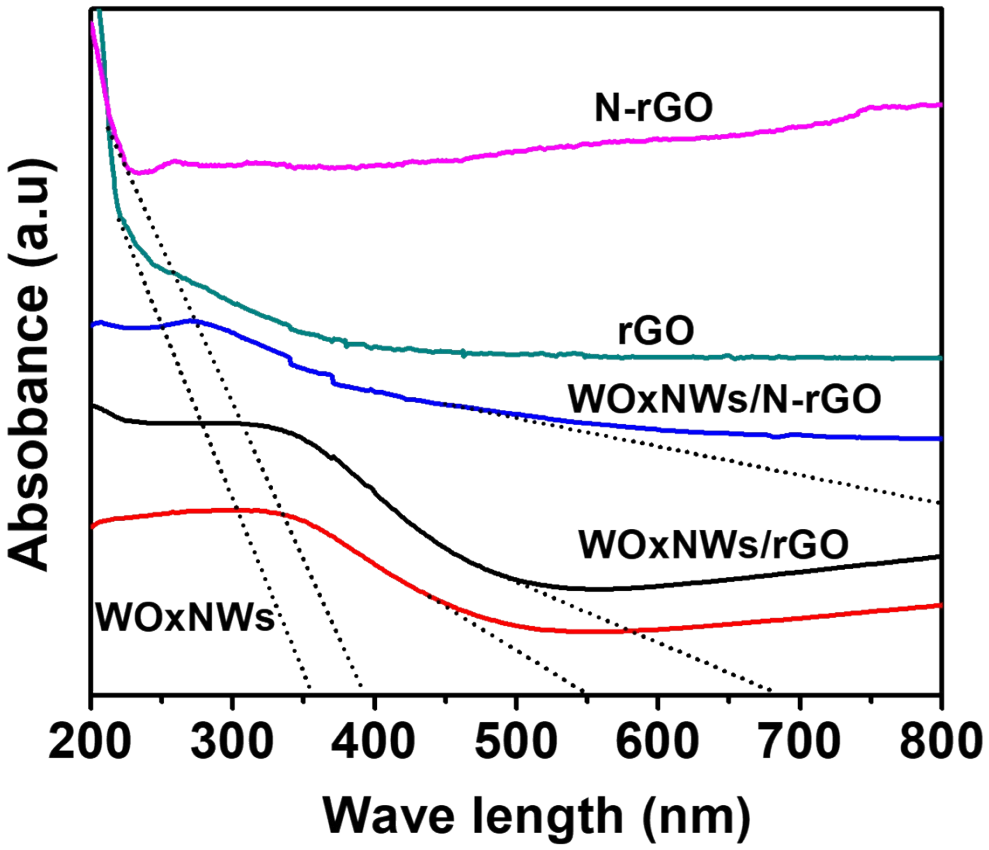

Figure S7 UV-Vis spectroscopy of WOxNWs,WOxNWs/rGO, WOxNWs/N-rGO, rGO and N-rGO

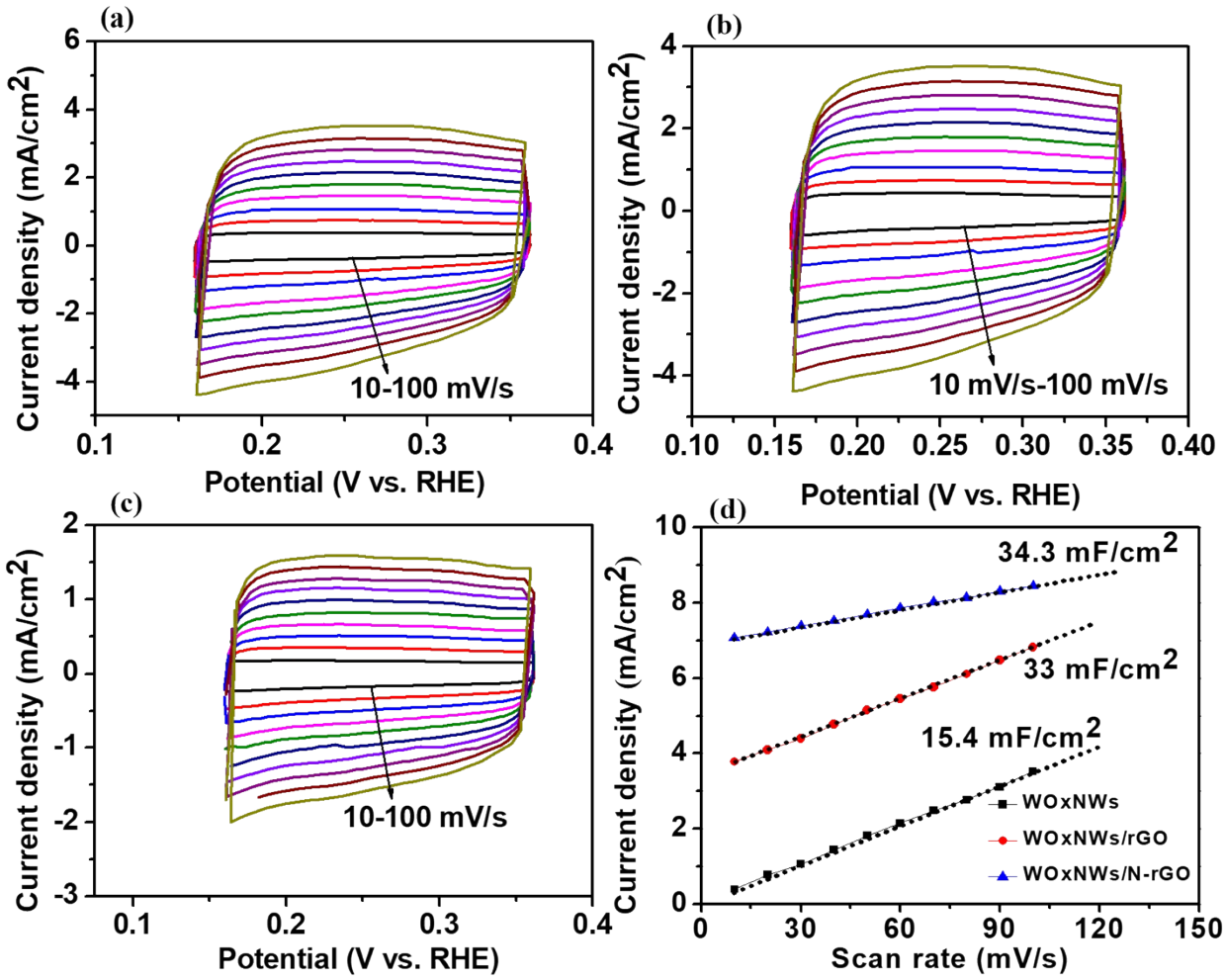

Figure S8 CV curves of (a) WOxNWs/N-rGO, (b) WOxNWs/rGO, and (c) WOxNWs at different scan rates; (d) current density vs. scan rates of different catalysts.

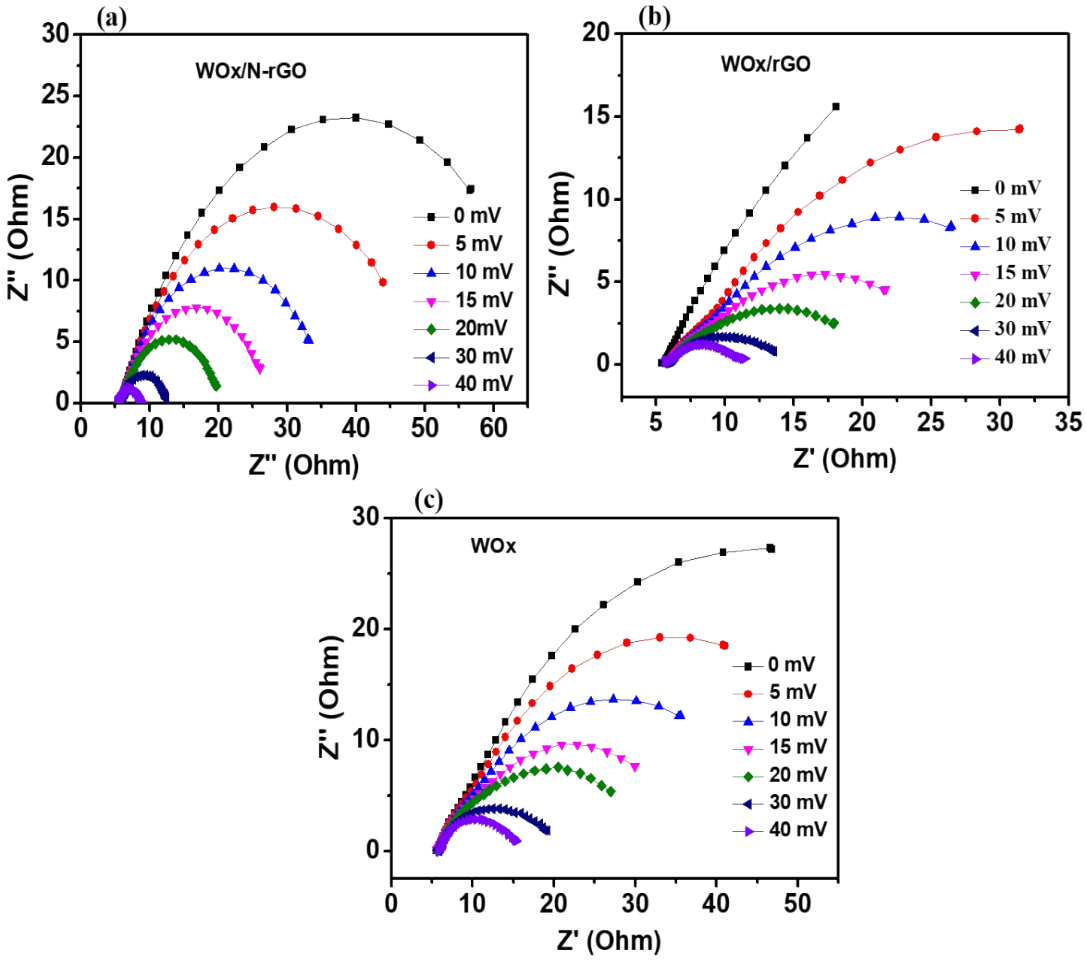

Figure S9 EIS spectra of (a)WOxNWs/N-rGO, (b) WOxNWs/rGO, and (c) WOxNWs at different overpotentials.

The morphology change before and after stability test is very important to understand robustness of the catalyst. The SEM image for WOxNWs/N-rGO before and after stability test is shown in **(Figure S10 (a and b)**. Accordingly, after 12 hours stability test in 0.5 M H_2SO_4 clearly shows that many nanowires are still existed and also seems aggregate. The aggregation might be due to the Nafion binder. Therefore, the catalyst is still robust in acidic media after long time stability test.

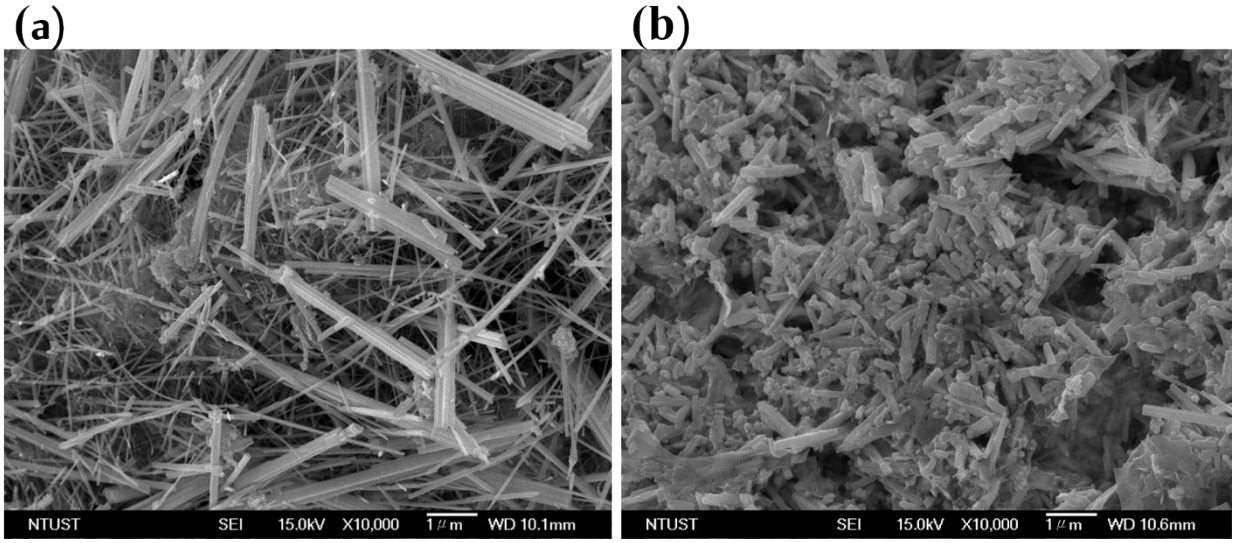

Figure S10 SEM image of WOxNWS/N-rGO (a) before and (b) after 12 h of stability test

In order to, further understand crystallinity, of the catalyst after 12 h stability test, XRD for WOxNWs/N-rGO was done by scratch from glassy carbon electrode (GCE) after stability test for several times. **Figure S11** is XRD pattern of WOxNWs/N-rGO before and after stability test and the peaks become a little bit broaden and (011) peak become intense this may be due to the decrease in particle size and leaching of carbon matrix from WOxNWs during stability measurement, respectively[1].

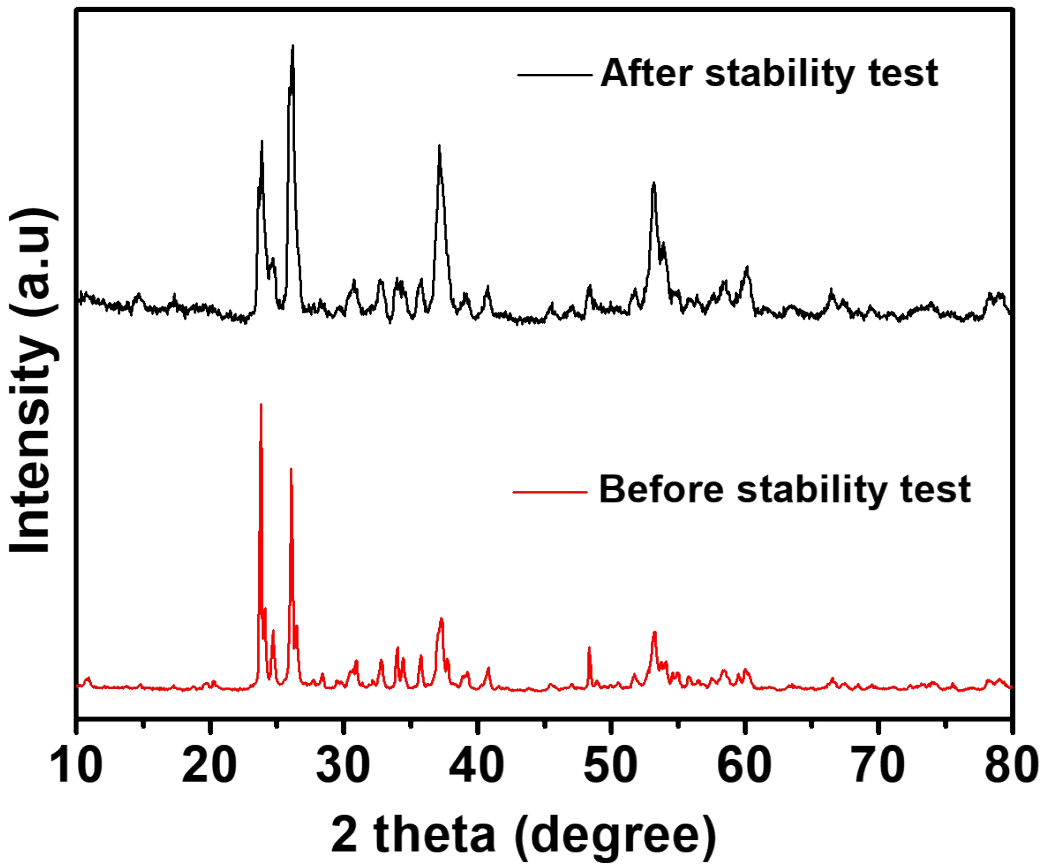

Figure S11 XRD pattern of WOxNWS/NrGO before stability test and after stability test

To understand the elemental composition after stability test XPS of WOxNWs/N-rGO have been done. **Figure S12 (a)** clearly shows that the existence of all elements after stability test and F1s intense peak is from Nafion binder because we use nafion to bind our catalyst on glassy carbon electrode . The N1s peak is very small, this may due to some carbon was leached after long time exposure in harsh acidic environment. The **Figure S12 (b)** is a narrow scan of tungsten before and after stability test and no obvious intensity decrease in the peaks indicates that tungsten after stability test are mainly WOxNWs. Moreover, no noticeable peak shift was observed on the W 4f XPS spectrum of after stability test in comparison to that of the fresh sample, suggesting the majority of O-vacancies are preserved during the HER.

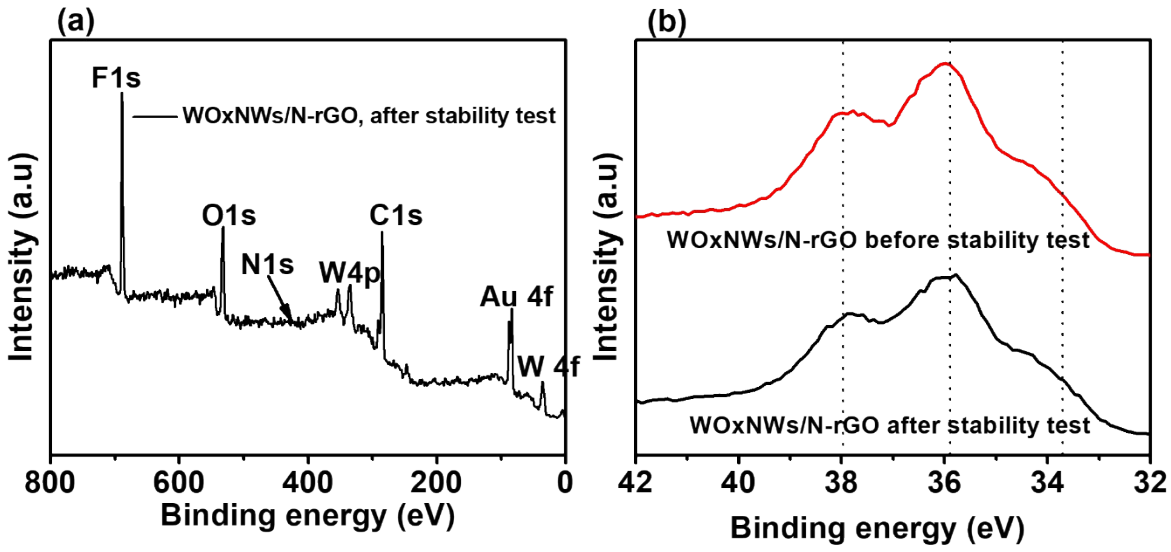

Figure S12 (a) XPS wide-scan sprectrum of WOxNWS/NrGO after stability test (b) XPS narrow-scan spectra of tungsten in WOxNWs/N-rGO before and after stability test.

Table S1 Summary of some tungsten-based and other non-precious metals catalyst for HER in 0.5 M H_2SO_4

Catalyst	mass loading (mg cm^{-2})	Tafel slope (mV dec^{-1})	Overpotential (mV) at 10 mA cm^{-2}	Exchange current density (mA cm^{-2})	Ref.
Fe@FeP/CNT	1.6	55	53	------	[2]
WON/CC	7.7	52	130	-------	[3]
WP/CC	2	69	125	0.29	[4]
$WO_{2.9}$	0.285	50	70	0.4	[5]
WO_2/W	2.2	74.5	120	--------	[6]
$WO_{(3-X)}$/ CNF	0.21	89	185	0.239	[7]
(MWCMNs)	0.35	46	58	0.46	[8]
P-WN/rGO	-------	54	85	0.35	[9]
W-Mo-O/rGO	0.12	46	50	-------	[10]
WS_2/SNC	0.36	66	96	-------	[11]
Mo-$W_{18}O_{49}$	0.16	54	-------	-------	[12]
WC/CC	-------	55	118	0.0165	[13]
$NiP_{1.93}Se_{0.07}$	--------	42	102	--------	[14]
CoS|P/CNTs	--------	55	64	---------	[15]
WOxNWs/N-rGO	0.51	38.2	40	1.46	This work

Notes and references:

[1] A. Fischer, M. Schmitz, B. Aichmayer, P. Fratzl, D. Faivre, Journal of The Royal Society Interface, (2011).

[2] X. Li, W. Liu, M. Zhang, Y. Zhong, Z. Weng, Y. Mi, Y. Zhou, M. Li, J.J. Cha, Z. Tang, H. Jiang, X. Li, H. Wang, Nano Lett, 17 (2017) 2057-2063.

[3] Q. Li, W. Cui, J. Tian, Z. Xing, Q. Liu, W. Xing, A.M. Asiri, X. Sun, ChemSusChem, 8 (2015) 2487-2491.

[4] Z. Pu, Q. Liu, A.M. Asiri, X. Sun, ACS Appl Mater Interfaces, 6 (2014) 21874-21879.

[5] Y.H. Li, P.F. Liu, L.F. Pan, H.F. Wang, Z.Z. Yang, L.R. Zheng, P. Hu, H.J. Zhao, L. Gu, H.G. Yang, Nat Commun, 6 (2015) 8064.

[6] Y. Zhao, C. Lv, Q. Huang, Z. Huang, C. Zhang, RSC Adv., 6 (2016) 89815-89820.

[7] J. Chen, D. Yu, W. Liao, M. Zheng, L. Xiao, H. Zhu, M. Zhang, M. Du, J. Yao, ACS Appl Mater Interfaces, 8 (2016) 18132-18139.

[8] R. Wu, J. Zhang, Y. Shi, D. Liu, B. Zhang, J Am Chem Soc, 137 (2015) 6983-6986.

[9] H. Yan, C. Tian, L. Wang, A. Wu, M. Meng, L. Zhao, H. Fu, Angew Chem Int Ed Engl, 54 (2015) 6325-6329.

[10] M. Imran, A.B. Yousaf, S.J. Zaidi, C. Fernandez, International Journal of Hydrogen Energy, 42 (2017) 8130-8138.

[11] J. Duan, S. Chen, B.A. Chambers, G.G. Andersson, S.Z. Qiao, Adv Mater, 27 (2015) 4234-4241.

[12] X. Zhong, Y. Sun, X. Chen, G. Zhuang, X. Li, J.-G. Wang, Advanced Functional Materials, 26 (2016) 5778-5786.

[13] B. Ren, D. Li, Q. Jin, H. Cui, C. Wang, Journal of Materials Chemistry A, 5 (2017) 13196-13203.

[14] J. Zhuo, M. Cabán-Acevedo, H. Liang, L. Samad, Q. Ding, Y. Fu, M. Li, S. Jin, ACS Catalysis, 5 (2015) 6355-6361.

[15] W. Liu, E. Hu, H. Jiang, Y. Xiang, Z. Weng, M. Li, Q. Fan, X. Yu, E.I. Altman, H. Wang, Nature Communications, 7 (2016) 10771.